

Room-Temperature Ferromagnetism in $(\text{Zn}_{1-x}\text{Mn}_x)\text{GeP}_2$ Semiconductors

Sunglae Cho,* Sungyoul Choi, Gi-Beom Cha, and Soon Cheol Hong

Department of Physics, University of Ulsan, Ulsan, 680-749, South Korea

Yunki Kim, Yu-Jun Zhao, Arthur J. Freeman, and John B. Ketterson

Department of Physics & Astronomy, Northwestern University, Evanston, Illinois 60208

B.J. Kim and Y.C. Kim

Department of Physics, Pusan National University, Busan, 609-735, South Korea

Byung-Chun Choi

Department of Physics, Pukyong National University, Busan, 609-737, South Korea

(Received 7 November 2001; published 6 June 2002)

We report on the discovery of a room-temperature ferromagnetic semiconductor in chalcopyrite $(\text{Zn}_{1-x}\text{Mn}_x)\text{GeP}_2$ with $T_c = 312$ K. We have also observed that, at temperatures below 47 K, samples for $x = 0.056$ and 0.2 show a transition to the antiferromagnetic (AFM) state, so that ferromagnetism is well defined to be present between 47 and 312 K. The observation that the AFM phase is most stable at low temperatures is consistent with the predictions of full-potential linearized augmented plane wave total energy calculations and has consequences for other chalcopyrite materials.

DOI: 10.1103/PhysRevLett.88.257203

PACS numbers: 75.50.Pp, 71.22.+i, 75.20.-g, 75.90.+w

The substitution of magnetic ions such as Mn^{2+} , Cr^{2+} , and Fe^{2+} into nonmagnetic semiconductors generates peculiar structural, electronic, electrical, optical, and magnetic properties. In the early work [1], II-VI semiconductors such as CdTe, CdSe, ZnSe, and ZnTe were widely studied since 2^+ magnetic ions can occupy the group-II cation sites of the host lattices. Concerning the magnetic properties, these systems usually showed antiferromagnetic (AFM) or spin glass ordering. III-V dilute magnetic semiconductors (DMSs) such as $(\text{InMn})\text{As}$ [2] and $(\text{GaMn})\text{As}$ [3,4] exhibited ferromagnetism; in this case, valence 2^+ Mn ions substitute on group III lattice sites and act as acceptors, generating hole concentrations of $\sim 10^{20} \text{ cm}^{-3}$. It is generally accepted that these hole carriers induce the ferromagnetic (FM) ordering in III-V systems. Recently, Medvedkin *et al.* [5] reported room-temperature ferromagnetism in unintentionally highly doped chalcopyrite $(\text{Cd}_{0.8}\text{Mn}_{0.2})\text{GeP}_2$. On the contrary, Zhao *et al.* [6] found that the total energy of the AFM state at $T = 0$ K is lower than the corresponding FM state for $\text{Cd}_{1-x}\text{Mn}_x\text{GeP}_2$ for $x = 1, 0.5$, and 0.25 using first principles full-potential linearized augmented plane wave (FLAPW) [7] and DMol³ [8] methods in the local-density approximation (LDA) and the generalized gradient approximation (GGA).

In this Letter, we report on the discovery of room-temperature FM ordering in electrically insulating $(\text{Zn}_{1-x}\text{Mn}_x)\text{GeP}_2$ and an AFM to FM transition at a temperature around 47 K. ZnGeP_2 , a II-IV-V₂ chalcopyrite semiconductor with a band gap of 2.0 eV at 300 K [9], is a tetrahedrally bonded ternary compound with a c/a ratio of 1.96, which crystallizes in a form that is “genealogically” related to the zinc-blende crystal structure; it is

gaining importance as a nonlinear optical material and has good transparency in the range of 0.7–12 μm . Nonlinear device applications include second-harmonic generation and optical parametric oscillators [10].

For single crystal and polycrystal $(\text{Zn}_{1-x}\text{Mn}_x)\text{GeP}_2$ preparation, we used high-purity (99.999%) zinc (Zn), germanium (Ge), manganese phosphide (Mn_3P_2), and phosphorus (P) powders as starting materials with a particle size of < -200 mesh. First, the powders were weighed and loaded into thick walled quartz ampoules. Then the ampoules were evacuated ($< 10^{-6}$ Torr) and sealed. After encapsulation, the sealed ampoule was mixed, loaded into a vertical furnace, and heated slowly to form single-phase $(\text{Zn}_{1-x}\text{Mn}_x)\text{GeP}_2$. The heating cycle was 50 °C/h to 530 °C, 24-h soak, 4 °C/h to 630 °C, 24-h soak, 20 °C/h to 1130 °C, 48 h soak [11]. For single crystal growth, the temperature was slowly cooled at 0.5 °C/h to a point below the melting temperature (1022 °C for ZnGeP_2) and thereafter at 100 °C/h. In single crystal growth, we have found that the maximum Mn concentration in $(\text{Zn}_{1-x}\text{Mn}_x)\text{GeP}_2$ corresponds to $x_{\text{max}} = 0.03$. We have prepared 8 mm \times 8 mm single crystals with $x = 0, 0.013$, and 0.03. Three polycrystalline samples with higher Mn concentrations, $x = 0.045, 0.056$, and 0.2, were prepared by furnace cooling after heat treatment at 1130 °C for 48 h. The Mn composition was determined using inductively coupled plasma spectroscopy.

In order to characterize the $(\text{Zn}_{1-x}\text{Mn}_x)\text{GeP}_2$ crystal structure, we performed Laue x-ray diffraction (XRD) studies on the single crystals and θ - 2θ powder diffraction on the polycrystalline samples. As shown in Fig. 1(a), the single crystal sample displays Laue spots, as expected for a single crystal. The polycrystalline samples show

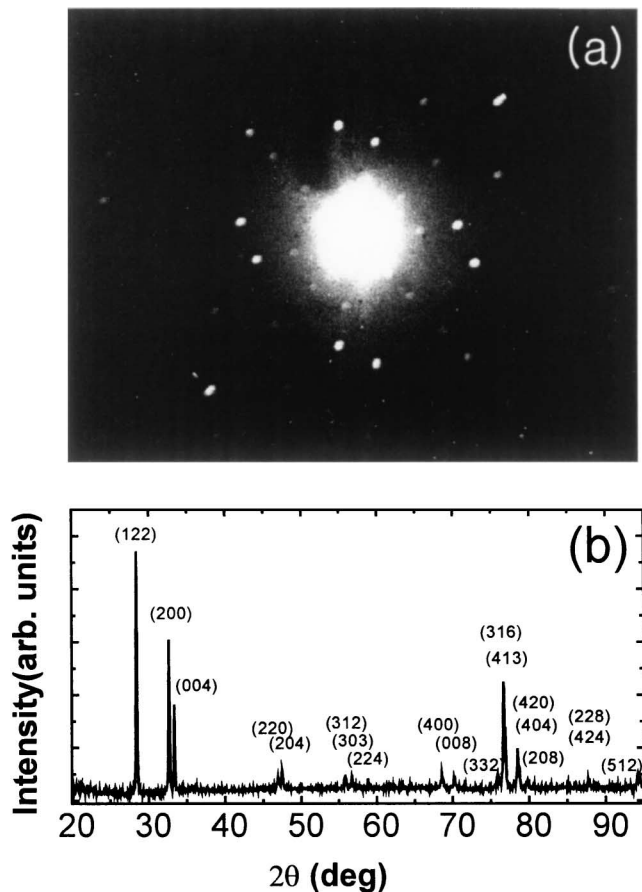


FIG. 1. (a) A Laue XRD pattern of a $(\text{Zn}_{0.97}\text{Mn}_{0.03})\text{GeP}_2$ single crystal. (b) The powder XRD pattern of polycrystalline $(\text{Zn}_{0.944}\text{Mn}_{0.056})\text{GeP}_2$, expected for a chalcopyrite crystal structure with no observable impurity peaks.

only $(\text{Zn}_{1-x}\text{Mn}_x)\text{GeP}_2$ diffraction peaks, which index with a tetrahedral chalcopyrite structure [Fig. 1(b)]. The lattice constants increase with Mn concentration, due to the larger Mn atomic radius (1.40 Å) than Zn (1.35 Å). The sample with $x = 0.056$ has lattice constants $a = 5.479$ Å and $c = 10.736$ Å, which are 0.34% larger than those of ZnGeP_2 ($a = 5.465$ Å, $c = 10.700$ Å). The addition of Mn into ZnGeP_2 induces a decrease in the energy gap, as determined in optical absorbance measurements at room temperature. As shown in Fig. 2, single crystalline $(\text{Zn}_{1-x}\text{Mn}_x)\text{GeP}_2$ for $x = 0.013$ and 0.03 has energy gaps of 1.9 and 1.83 eV, respectively, which is smaller than that of ZnGeP_2 , 2.0 eV [9].

We have investigated the magnetic properties on these samples using a SQUID (superconducting quantum interference device, Quantum Design) magnetometer. Figure 3(a) shows the temperature-dependent magnetization (M) of $(\text{Zn}_{1-x}\text{Mn}_x)\text{GeP}_2$ single crystals and polycrystals with $x = 0.013, 0.03, 0.045, 0.056,$ and 0.2 between 5 and 400 K in a 100 Oe magnetic field. The magnetization of the single crystal with $x = 0.013$ shows a transition at 312 K and increases rapidly as temperature decreases in the region below 100 K. With increasing Mn content ($x = 0.03$ and 0.045), there is a drop in the magnetiza-

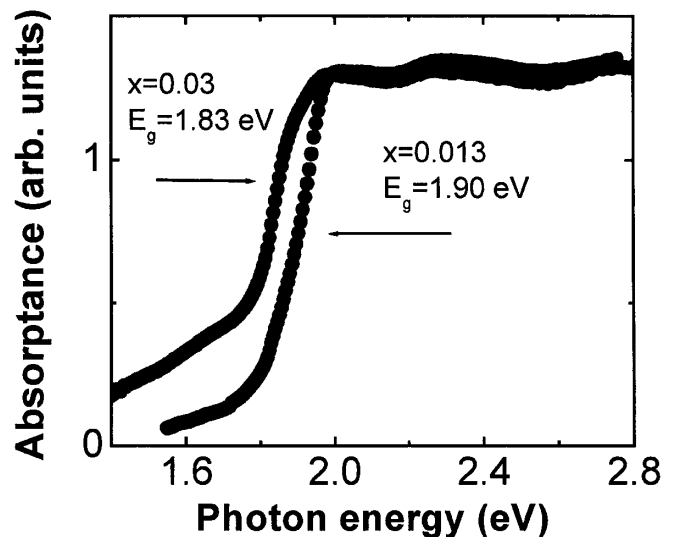


FIG. 2. Optical absorption of $(\text{Zn}_{1-x}\text{Mn}_x)\text{GeP}_2$ single crystals with $x = 0.013$ and 0.03 at room temperature. Note that the energy gap of ZnGeP_2 is 2.0 eV at 300 K.

tion around 47 K after which it again increases. However, for $x = 0.056$ and 0.2, the low temperature increase in the magnetization disappears; there are now two quite distinct transitions at 47 and 312 K.

M - H curves of a $(\text{Zn}_{0.97}\text{Mn}_{0.03})\text{GeP}_2$ single crystal at 5, 100, 250, 280, and 350 K are shown in Fig. 3(b). At 5 and 350 K, the crystal shows a linear M vs H dependence, characteristic of paramagnetic (PM) states. Below 312 K and above about 47 K, this sample is FM. The coercivity field is 23 Oe at 250 K, as shown in the inset. Figure 3(c) shows M - H curves of the polycrystalline $(\text{Zn}_{0.944}\text{Mn}_{0.056})\text{GeP}_2$ sample at 5, 100, 250, 280, and 350 K. A similar PM-FM phase transition is seen at 312 K. Between ~ 47 and 312 K, this crystal also shows FM behavior. The 5 K data, which now show a small initial slope followed by a rapid rise after which saturation sets in, are consistent with an AFM low field state, the rapid rise then being interpreted as a spin-flop transition. Hence, we identify the 47 K transition as an AFM to FM transition.

The magnetic moment per Mn atom at different temperatures for $x = 0.056$ is shown in the inset of Fig. 3(c), showing that the PM-FM phase transition occurs at 312 K; the magnetic moment rises rapidly down to 280 K, and saturates thereafter. The moment per Mn at 2 K for $x = 0.056$ and 0.2 is $3.85\mu_B$ and $4.9\mu_B$, respectively. These values are larger than those of DMSS; $2.3\mu_B, 2\mu_B, 0.32\mu_B,$ and $0.3\mu_B$ for $\text{Ga}_{1-x}\text{Mn}_x\text{As}$ [3], $\text{Zn}_{1-x}\text{Co}_x\text{O}$ [12], $\text{Ti}_{1-x}\text{Co}_x\text{O}_2$ [13], and $\text{Ga}_{1-x}\text{Mn}_x\text{N}$ [14], respectively.

The magnetization measured in a field of 100 Oe increased rapidly with Mn concentration (x) up to $x = 0.056$. This above-linear increase of M vs Mn content (x) at low concentrations may arise from large fluctuations in the Mn concentration in ZnGeP_2 . For lightly Mn-doped samples ($x = 0.013$), it is assumed that the substituted

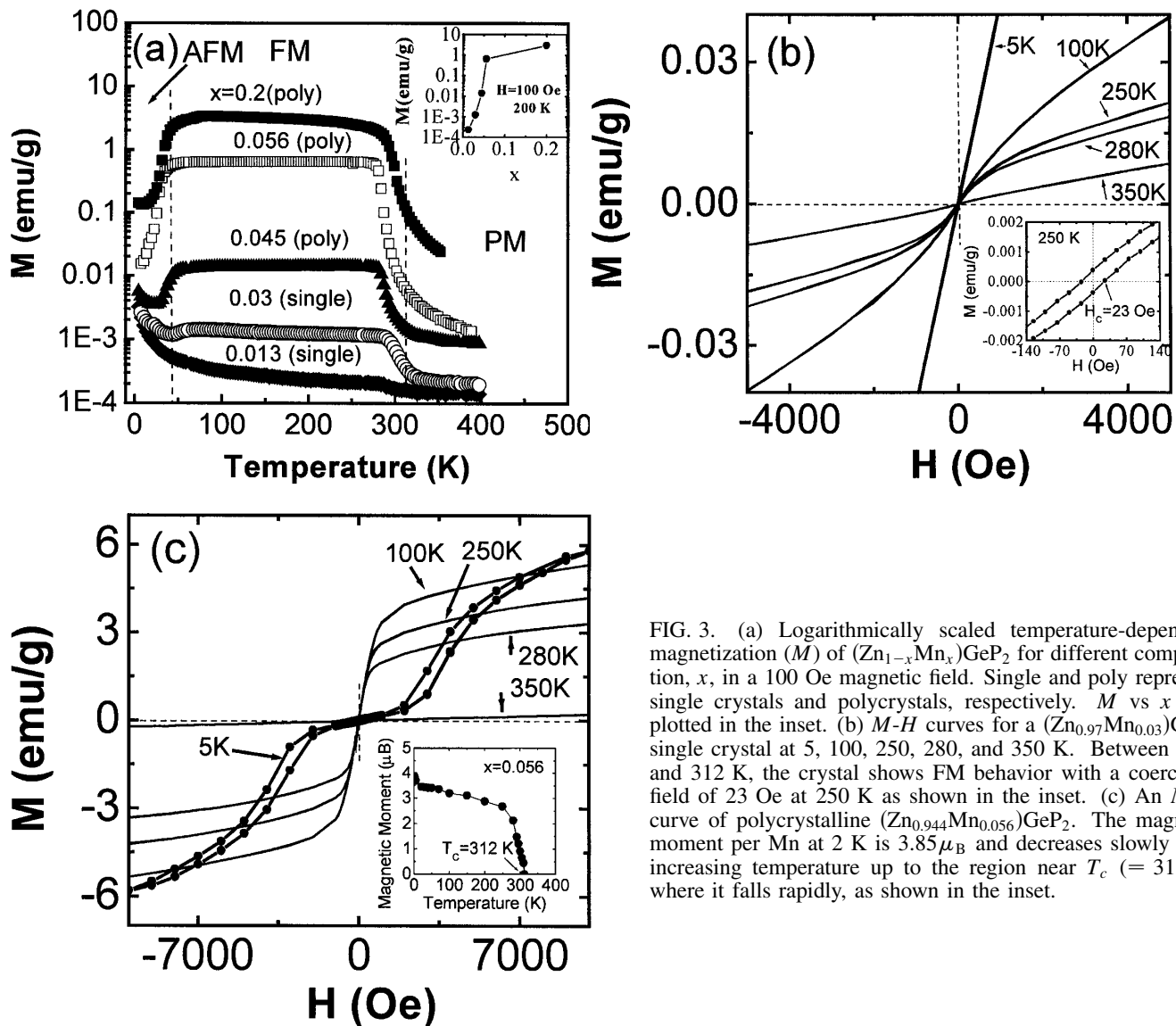


FIG. 3. (a) Logarithmically scaled temperature-dependent magnetization (M) of $(\text{Zn}_{1-x}\text{Mn}_x)\text{GeP}_2$ for different composition, x , in a 100 Oe magnetic field. Single and poly represent single crystals and polycrystals, respectively. M vs x was plotted in the inset. (b) M - H curves for a $(\text{Zn}_{0.97}\text{Mn}_{0.03})\text{GeP}_2$ single crystal at 5, 100, 250, 280, and 350 K. Between ~ 47 and 312 K, the crystal shows FM behavior with a coercivity field of 23 Oe at 250 K as shown in the inset. (c) An M - H curve of polycrystalline $(\text{Zn}_{0.944}\text{Mn}_{0.056})\text{GeP}_2$. The magnetic moment per Mn at 2 K is $3.85\mu_B$ and decreases slowly with increasing temperature up to the region near T_c ($= 312$ K) where it falls rapidly, as shown in the inset.

Mn ions are too widely separated to order (i.e., isolated), resulting in a predominantly PM state with a slight change at around 312 K. With increasing Mn content ($x = 0.03$ and 0.045), both PM and AFM phases are present at low temperatures, indicating the presence of dilute (PM-like) and dense (AFM-like) Mn regions. Compositions with $x \geq 0.056$ show only an AFM phase at low temperature; here it is presumed that the Mn distribution is such that regions with closely spaced, possibly ordered, Mn ions are present (likely occupying the Zn sites). Similar spatial fluctuations of the Mn concentration were reported in ZnTe based on a neutron scattering experiment [1]. From these observations, we may conclude that the Mn ions in ZnGeP_2 do not substitute uniformly but fluctuate spatially.

In order to microscopically understand the observed magnetism of $(\text{Zn}_{1-x}\text{Mn}_x)\text{GeP}_2$, we carried out first principles electronic structure calculations, using the FLAPW and DMol³ methods in both the LDA and the GGA. Table I presents the calculated total energy difference between AFM and FM states and magnetic

moments for $x = 0.25, 0.5$, and 1.0 . As shown in Table I, AFM ordering at 0 K is energetically favorable, relative to the FM state. The calculated total energy is consistent with the experimental observation of AFM ordering at low temperature. The spin only contribution to the magnetic moments was calculated to be $5.0\mu_B$, $4.91\mu_B$, and $3.24\mu_B$ for $x = 0.25, 0.5$, and 1.0 , respectively, and appears to be in reasonable agreement with the full experimental moment ($4.9\mu_B$) for $x = 0.2$ derived from the saturation magnetization.

Note that both single-crystal and polycrystalline samples were electrically insulating since Mn^{2+} can readily be substituted for the group II cation, Zn, without the formation of structural defects, owing to the natural tendency of Mn to adopt a 2+ state. In III-V based DMS such as GaMnAs and InMnAs, the addition of Mn^{2+} into the group III cation sites generates holes, as mentioned earlier [2–4]. These induced hole carriers are thought to mediate the interaction of the magnetic ions, resulting in the FM state. However, in our systems, *no carriers are*

TABLE I. The energy difference between FM and AFM ($Zn_{1-x}Mn_x$)GeP₂ for $x = 0.25, 0.5$, and 1.0 and corresponding magnetic moment. The linear interpolated lattice constant from experimental ZnGeP₂ values and "conservation of tetrahedral bonds plus $\eta = \eta_{tet}$ " values [6] for MnGeP₂ are employed, and internal structures are fully optimized.

x	$\Delta E = E_{AFM} - E_{FM}$ (meV/Mn)				Total magnetic moment in FM state (μ_B /Mn)	
	DMol ³		FLAPW		FLAPW	
	LDA	GGA	LDA	GGA	LDA	GGA
0.25	-58	-38	-64	-45	5.0	5.0
0.50	-34	-31	-30	-26	4.91	4.99
1.00	-165	-258	-159	-248	3.24	4.52

induced with the addition of Mn into Zn sites. Our results appear to call into question the necessity of having holes to generate ferromagnetic coupling in zinc-blende-based semiconductors. Note that the electrically insulating Eu chalcogenides such as EuO and EuS, which have rock salt structure, showed ferromagnetic ordering at $T_c = 69$ and 17 K, respectively [15].

We have performed doping experiments on ($Zn_{0.92}Mn_{0.08}$)GeP₂ polycrystals. It is well known that In, Ga, and Se [16] are p -type dopants for ZnGeP₂, while an n -type dopant has not been reported. In this study, we used Te as a p -type dopant with a carrier concentration of $\sim 10^{16} \text{ cm}^{-3}$ at room temperature, determined by a Hall measurement and also verified with a thermopower measurement. Figure 4 shows the temperature-dependent resistance on a logarithmic scale between 5 and 400 K in zero magnetic field. The resistance increases with decreasing temperature. Note that we can see two distinct slope changes in resistance at around 47 and 312 K, corresponding to AFM-FM and FM-PM phase transitions, respectively. A similar resistance slope change is observed at the phase transition temperature in GaMnAs due to the changes in spin-related scattering and conduction mechanisms [17]. Thus, the temperature-dependent resistance results strongly support the presence of phase transitions (AFM-FM and FM-PM) at around 47 and 312 K, respectively. This finding may resolve the apparent disagreement between observations [5] at room temperature and density functional predictions [6] at $T = 0$ for ($Cd_{1-x}Mn_x$)GeP₂.

In conclusion, we have observed room-temperature ferromagnetism and an AFM-FM transition around 47 K in a chalcopyrite-based semiconductor. The observation that the AFM phase is most stable at low temperatures is consistent with the predictions of FLAPW total energy calculations and has consequences for other chalcopyrite materials. It is plausible that this and related materials can replace the Mn doped III-V systems and open the way to room temperature spintronic devices.

We gratefully acknowledge significant discussions with J. Furdyna from which several of the ideas underlying the present work evolved. This work is supported by KOSEF Excellence Program through ASSRC at Yonsei

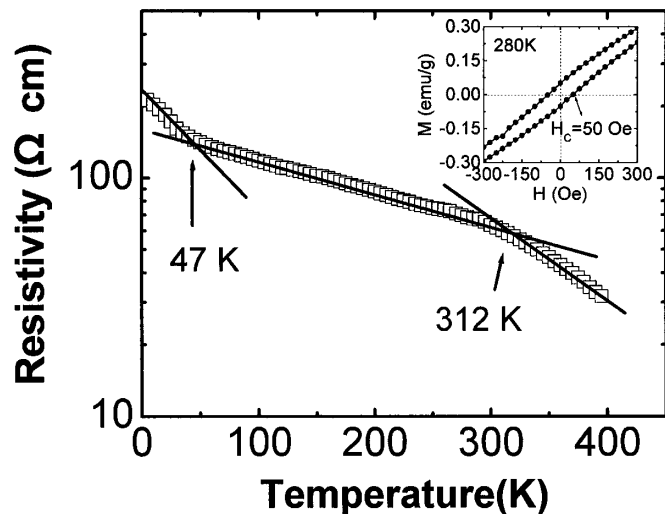


FIG. 4. Logarithmically scaled temperature-dependent resistivity of a Te-doped ($Zn_{0.92}Mn_{0.08}$)GeP₂ polycrystalline sample under zero magnetic field. There are changes in slope at ~ 47 and 312 K, corresponding to the AFM-FM and FM-PM transitions, respectively. The coercivity of this sample was 50 Oe at 280 K, as shown in the inset.

University. Research at Northwestern was supported by the ONR/Durip under Award No. N00014-01-1-0438, the AFOSR Chalcopyrite MURI under Grant No. F49720-01-1-0428, and Materials Research Center under the National Science MERSEC program.

*Email address: slcho@mail.ulsan.ac.kr

- [1] J. K. Furdyna, J. Appl. Phys. **64**, R29 (1988).
- [2] H. Ohno, H. Munekata, T. Penny, S. van Molnár, and L. L. Chang, Phys. Rev. Lett. **68**, 2664 (1992).
- [3] H. Ohno, Science **281**, 951 (1998).
- [4] T. Dietl, H. Ohno, F. Matsukura, J. Cibert, and D. Ferrand, Science **287**, 1019 (2000).
- [5] G. A. Medvedkin *et al.*, Jpn. J. Appl. Phys. **39**, L949 (2000).
- [6] Yu-Jun Zhao, W. T. Geng, A. J. Freeman, and T. Oguchi, Phys. Rev. B **63**, 201202 (2001).
- [7] E. Wimmer, H. Krakauer, M. Weinert, and A. J. Freeman, Phys. Rev. B **24**, 864 (1981).
- [8] B. Delley, J. Chem. Phys. **113**, 7756 (2000).
- [9] V. Yu. Rud' and Yu. V. Rud', Tech. Phys. Lett. **23**, 415 (1997).
- [10] G. C. Bhar, S. Das, U. Chatterjee, and K. L. Vodopyanov, Appl. Phys. Lett. **54**, 313 (1989).
- [11] B. Ray, A. J. Pyane, and G. J. Burnell, Phys. Status Solidi A **35**, 197 (1969).
- [12] K. Ueda, H. Tabata, and T. Kawai, Appl. Phys. Lett. **79**, 988 (2001).
- [13] Y. Matsumoto *et al.*, Science **291**, 854 (2001).
- [14] M. E. Overberg *et al.*, Appl. Phys. Lett. **79**, 1312 (2001).
- [15] W. Notting, Phys. Status Solidi (b) **96**, 11 (1979).
- [16] B. H. Bairamov, V. Yu. Rud', and Yu. V. Rud', MRS Bull. **23**, 41 (1998).
- [17] A. Van Esch *et al.*, Phys. Rev. B **56**, 13 103 (1997).